On the evolution of tachyonic perturbations at super-Hubble scales

Rajeev Kumar Jain
Harish-Chandra Research Institute, Chhatnag Road, Jhunsi, Allahabad 211 019, India.
E-mail: rajeev@mri.ernet.in

Pravabati Chingangbam
Korea Institute for Advanced Study, 207–43 Cheongnyangni 2-dong, Dongdaemun-gu, Seoul 130-722, Korea.
E-mail: prava@kias.re.kr

L. Sriramkumar
Harish-Chandra Research Institute, Chhatnag Road, Jhunsi, Allahabad 211 019, India.
E-mail: sriram@mri.ernet.in

Abstract. In the slow-roll inflationary scenario, the amplitude of the curvature perturbations approaches a constant value soon after the modes leave the Hubble radius. However, relatively recently, it was shown that the amplitude of the curvature perturbations induced by the canonical scalar field can *grow* at super-Hubble scales if there is either a transition to fast roll inflation or if inflation is interrupted for some period of time. In this work, we extend the earlier analysis to the case of a non-canonical scalar field described by the Dirac-Born-Infeld action. With the help of a specific example, we show that the amplitude of the tachyonic perturbations can be *enhanced or suppressed* at super-Hubble scales if there is a transition from slow roll to fast roll inflation. We also illustrate as to how the growth of the entropy perturbations during the fast roll regime proves to be responsible for the change in the amplitude of the curvature perturbations at super-Hubble scales. Furthermore, following the earlier analysis for the canonical scalar field, we show that the power spectrum evaluated in the long wavelength approximation matches the exact power spectrum obtained numerically very well. Finally, we briefly comment on an application of this phenomenon.

PACS numbers: 98.80.Cq

1. Introduction

It is well-known that, in the inflationary scenario, the amplitude of the curvature perturbations approaches a constant value soon after the modes leave the Hubble radius (see, for example, either of the following texts [1] or one of the following reviews [2]). But, what is not so commonly known is that this result is true *only* in slow roll or power law inflation and, in fact, the curvature perturbations can be amplified at super-Hubble scales if there is either a period of fast roll inflation or if there is a break in inflation. For the case of curvature perturbations induced by the canonical scalar field, this behavior was first noticed a few years back [3] and a general criterion for such an amplification to occur was also obtained [4]. Our aim in this work is to extend the earlier analysis [3, 4] to the case of curvature perturbations generated by a non-canonical scalar field. Interestingly, we find that, in addition to enhancing the amplitude of the curvature perturbations of a certain range of modes at super-Hubble scales, a period of deviation from slow roll inflation also leads to the suppression of the amplitude of another range of modes.

The non-canonical scalar field that we shall consider is the one that is described by the Dirac-Born-Infeld (DBI, hereafter) action. Such scalar fields generically arise in the study of the dynamics of D-branes in string theory [5]. In particular, the tachyon, which refers to an unstable DBI scalar field that rolls down from the maxima of its potential near the origin to its minima at infinity, captures the essential dynamical features of the decay process of unstable branes (for the original discussion, see Refs. [6]). Various cosmological applications of the tachyon have been studied extensively in the literature (see, for instance, Refs. [7] and references therein) and, in particular, it has proved to be a fertile ground for inflationary model building (see, for example, Ref. [8] and references therein). It is also possible to have DBI scalar fields whose potential has a global minimum at the origin so that the field rolls down from a large value towards the origin (see, for example, Ref. [9]; for cosmological applications of such fields, see, for instance, Refs. [10]). We shall consider such a scenario in this work. It should be pointed out here that the DBI scalar field falls under a broader class of non-canonical scalar field models that are often referred to as the k-inflation models [11].

With the help of a specific example, we shall illustrate that the amplitude of the curvature perturbations induced by the DBI scalar field can be enhanced or suppressed (when compared to its value at Hubble exit) at super-Hubble scales if there is a period of deviation from slow roll inflation. We shall also show that it is the growth of entropy perturbations during such a transition that turns out to be responsible for the change in the amplitude of the tachyonic perturbations‡. Moreover, following the earlier analysis

‡ Actually, as we mentioned above, the term 'tachyon' refers to a DBI scalar field that is described by a potential with a maxima near the origin. The specific potential we shall consider in this paper does not have this feature. Nevertheless, we shall often use the terms 'tachyon' and 'tachyonic perturbations' as convenient shorthands for referring to the DBI scalar field and to the perturbations induced by it, respectively.

for the canonical scalar field, we shall show that the power spectrum evaluated in the long wavelength approximation and the exact power spectrum obtained numerically match rather well. We shall also very briefly comment on an interesting application of this phenomenon.

The remainder of this paper is organized as follows. In the following section, we shall briefly summarize the essential background equations and the equations describing the scalar perturbations generated by the DBI scalar field. In Section 3, we shall illustrate the amplification or suppression of the curvature perturbations at super-Hubble scales when there is a transition from slow roll to fast roll and back with the help of a specific example. We shall also show as to how the entropy perturbations grow during the period of fast roll inflation which in turn act as the source for the evolution of the curvature perturbations at super-Hubble scales. In Section 4, we extend an earlier result for the canonical scalar field to the tachyonic case and show that the power spectrum calculated in the long wavelength approximation agrees quite well with the exact power spectrum evaluated numerically. Finally, in Section 5, we close by commenting on an important application of our result.

Before we proceed further, a few words on the conventions and notations we shall adopt are in order. We shall set $\hbar = c = 1$ and work with the metric signature of $(+,-,-,-)$. We shall express the various quantities in terms of either the cosmic time t or the conformal time η, as is convenient. An overdot shall denote differentiation with respect the cosmic time and an overprime shall denote differentiation with respect to the conformal time. It is useful to note here that, for any given function, say, f, $\dot{f} = (f'/a)$ and $\ddot{f} = [(f''/a^2) - (f'\,a'/a^3)]$, where a is the scale factor describing the Friedmann background.

2. Essential results from cosmological perturbation theory

In this section, we shall briefly outline essential cosmological perturbation theory. We shall quickly summarize the equations describing the Friedmann background and the tachyonic perturbations that we will require for our discussion.

2.1. The background equations

Consider a $(3+1)$-dimensional, spatially flat, smooth, Friedmann universe described by line element

$$ds^2 = dt^2 - a^2(t)\, d\mathbf{x}^2 = a^2(\eta)\, \left(d\eta^2 - d\mathbf{x}^2\right), \tag{1}$$

where t is the cosmic time, $a(t)$ is the scale factor and $\eta = \int dt/a(t)$ denotes the conformal time. If ρ and p denote the energy density and the pressure of the smooth component of the matter field that is driving the expansion, then the Einstein's equations for the above line-element lead to the following Friedmann equations for the scale factor $a(t)$:

$$\left(\frac{\dot{a}}{a}\right)^2 = \left(\frac{8\pi\, G}{3}\right)\, \rho \qquad \text{and} \qquad \left(\frac{\ddot{a}}{a}\right) = -\left(\frac{4\pi\, G}{3}\right)\, (\rho + 3\, p)\,. \tag{2}$$

For the case of a DBI scalar field, say, T, described by the potential $V(T)$, the background energy density ρ and pressure p are given by

$$\rho = \left(\frac{V(T)}{\sqrt{1-\dot{T}^2}}\right) \qquad \text{and} \qquad p = -\left(V(T)\, \sqrt{1-\dot{T}^2}\right). \tag{3}$$

Also, in the spatially flat, Friedmann background that we shall be considering, the equation of motion for the tachyon T is given by

$$\left(\frac{\ddot{T}}{1-\dot{T}^2}\right) + (3\, H)\, \dot{T} + \left(\frac{V_T}{V}\right) = 0, \tag{4}$$

where $H = (\dot{a}/a)$ denotes the Hubble parameter and $V_T \equiv (dV/dT)$.

2.2. The scalar perturbations

2.2.1. Generic results If we now take into account the scalar perturbations to the background metric (1), then the Friedmann line-element, in general, can be written as [1, 2, 12]

$$\mathrm{d}s^2 = a^2(\eta)\, \left[(1+2A)\, \mathrm{d}\eta^2 - 2\, (\partial_i B)\, \mathrm{d}x^i\, \mathrm{d}\eta - ((1-2\psi)\, \delta_{ij} + 2\, \partial_i\partial_j E)\, \mathrm{d}x^i\, \mathrm{d}x^j\right], \tag{5}$$

where A, B, ψ and E are the scalar functions that describe the perturbations. The two gauge-invariant Bardeen variables that characterize the two degrees of freedom describing the scalar perturbations are given by [1, 2, 12]

$$\Phi \equiv A + \left(\frac{1}{a}\right)\, [(B-E')\, a]' \qquad \text{and} \qquad \Psi \equiv \psi - \mathcal{H}\, (B - E')\,. \tag{6}$$

In the absence of anisotropic stresses, as it is in the case of the scalar field sources that we are interested in, it can be readily shown that, at the linear order in the perturbations, the non-diagonal component of the Einstein equations leads to the relation: $\Phi = \Psi$. The remaining first order Einstein equations then reduce to [1, 2, 12]

$$\nabla^2\Phi - 3\, \mathcal{H}\, (\Phi' + \mathcal{H}\, \Phi) = \left(4\pi G\, a^2\right)\, [\delta\rho + \rho'\, (B - E')]\,, \tag{7}$$

$$\partial_i\, (\Phi' + \mathcal{H}\, \Phi) = \left(4\pi G\, a^2\right)\, [\delta q_i + (\rho + p)\, \partial_i\, (B - E')]\,, \tag{8}$$

$$\Phi'' + 3\, \mathcal{H}\, \Phi' + \left(2\, \mathcal{H}' + \mathcal{H}^2\right)\, \Phi = \left(4\pi G\, a^2\right)\, [\delta p + p'\, (B - E')]\,, \tag{9}$$

where $\mathcal{H} = (H\, a)$ is the conformal Hubble parameter, and $\delta\rho$, δq_i and δp denote the perturbations at the linear order in the energy density, flux, and the pressure of the matter field, respectively. The first and the third of the above first order Einstein equations can be combined to lead to the following differential equation for the Bardeen potential Φ [1, 2, 12]:

$$\Phi'' + 3\, \mathcal{H}\, \left(1 + c_{_\mathrm{A}}^2\right)\, \Phi' - c_{_\mathrm{A}}^2\, \nabla^2\Phi + \left[2\, \mathcal{H}' + \left(1 + 3\, c_{_\mathrm{A}}^2\right)\, \mathcal{H}^2\right]\, \Phi = (4\pi G)\, a^2\, \delta p_{_\mathrm{NA}}, \tag{10}$$

where we have made use of the standard relation

$$\delta p = c_{_{\rm A}}^2\, \delta\rho + \delta p_{_{\rm NA}}, \tag{11}$$

with $c_{_{\rm A}}^2 \equiv (p'/\rho')$ denoting the adiabatic speed of sound and $\delta p_{_{\rm NA}}$ representing the non-adiabatic pressure component. The quantity $\delta p_{_{\rm NA}}$ is usually related to the entropy perturbation $\mathcal{S}$§ as follows (see, for instance, Ref. [13]):

$$\delta p_{_{\rm NA}} = \left(\frac{p'}{\mathcal{H}}\right)\, \mathcal{S}. \tag{12}$$

The curvature perturbation $\mathcal{R}$ is defined in terms of the Bardeen potential Φ as [2]

$$\mathcal{R} = \Phi + \left(\frac{2\,\rho}{3\,\mathcal{H}}\right)\, \left(\frac{\Phi' + \mathcal{H}\,\Phi}{\rho + p}\right). \tag{13}$$

On substituting this expression for the curvature perturbation in the equation (10) describing the evolution of the potential Φ and making use of the background equations, we obtain that [13]

$$\mathcal{R}' = -\left(\frac{\mathcal{H}}{\mathcal{H}' - \mathcal{H}^2}\right)\, \left[\left(\frac{4\pi G\, a^2\, p'}{\mathcal{H}}\right)\, \mathcal{S} + c_{_{\rm A}}^2\, \nabla^2\Phi\right]. \tag{14}$$

2.2.2. For the tachyonic case To begin with, if we denote the perturbation in the DBI scalar field as δT, then, it is straightforward to show that, the perturbations in the energy density, the momentum flux and the pressure of the scalar field are given by

$$\delta\rho = \left(\frac{V_T\, \delta T}{\sqrt{1 - \dot{T}^2}}\right) + \left(\frac{V\, \dot{T}}{\left(1 - \dot{T}^2\right)^{3/2}}\right)\, \left(\dot{\delta T} - A\, \dot{T}\right), \tag{15}$$

$$\delta q_i = \left(\frac{V\, \dot{T}}{a\, \sqrt{1 - \dot{T}^2}}\right) (\partial_i\, \delta T), \tag{16}$$

$$\delta p = -\left(V_T\, \delta T\, \sqrt{1 - \dot{T}^2}\right) + \left(\frac{V\, \dot{T}}{\sqrt{1 - \dot{T}^2}}\right)\, \left(\dot{\delta T} - A\, \dot{T}\right), \tag{17}$$

where A is the quantity that appears in the perturbed Friedmann line-element (5). On substituting these expressions for $\delta\rho$, δq_i and δp in the first order Einstein equations (7)–(9), we find that the Bardeen potential Φ induced by the tachyonic perturbations satisfies the following differential equation:

$$\Phi'' + 3\,\mathcal{H}\, \left(1 + c_{_{\rm A}}^2\right)\, \Phi' - c_{_{\rm A}}^2\, \nabla^2\Phi + \left[2\,\mathcal{H}' + \left(1 + 3\, c_{_{\rm A}}^2\right)\, \mathcal{H}^2\right]\, \Phi = \left(c_{_{\rm S}}^2 - c_{_{\rm A}}^2\right)\, \nabla^2\Phi, \tag{18}$$

where $c_{_{\rm S}}^2 = (1 - \dot{T}^2)$ is referred to as the effective speed of sound (see, for instance, Ref. [14]). If we now compare the above equation with Eq. (10) and make use of the relation (12), we obtain the corresponding entropy perturbation to be [14]

$$\mathcal{S} = \left(\frac{\mathcal{H}}{4\pi G\, a^2\, p'}\right)\, \left(c_{_{\rm S}}^2 - c_{_{\rm A}}^2\right)\, \nabla^2\Phi. \tag{19}$$

§ The quantities that appear within the square brackets on the right hand sides of the first order Einstein equations (7) and (9) are the gauge-invariant versions of $\delta\rho$ and δp. On using these expressions in the relation (11), it is straightforward to show that $\delta p_{_{\rm NA}}$ and, therefore, $\mathcal{S}$ are gauge-invariant.

Therefore, for the tachyonic case, the equation (14) describing the evolution of the curvature perturbation simplifies to

$$\mathcal{R}' = -\left(\frac{4\pi G\, a^2\, p'}{\mathcal{H}' - \mathcal{H}^2}\right)\, \left(\frac{c_{\rm S}^2}{c_{\rm S}^2 - c_{\rm A}^2}\right)\, \mathcal{S} = -\left(\frac{\mathcal{H}\, c_{\rm S}^2}{\mathcal{H}' - \mathcal{H}^2}\right)\, \nabla^2\Phi. \tag{20}$$

On making use of this relation alongwith the definition (13) and the equation (18) describing the evolution of the Bardeen potential, we find that the Fourier modes of the curvature perturbation induced by the DBI scalar field are described by the differential equation

$$\mathcal{R}_k'' + 2\,\left(\frac{z'}{z}\right)\, \mathcal{R}_k' + k^2\, c_{\rm S}^2\, \mathcal{R}_k = 0, \tag{21}$$

where the quantity z is given by

$$z = \left(\frac{a}{H}\right)\, \left(\frac{\rho + p}{c_{\rm S}^2}\right)^{1/2} = \left(\frac{\sqrt{3}\, M_{\rm P}\, a\, \dot{T}}{\sqrt{1 - \dot{T}^2}}\right) \tag{22}$$

and $M_{\rm P} = (8\pi G)^{-1/2}$ denotes the Planck mass. The scalar power spectrum is then defined as

$$\mathcal{P}_{\rm S}(k) = \left(\frac{k^3}{2\,\pi^2}\right)\, |\mathcal{R}_{\rm k}|^2 \tag{23}$$

with the amplitude of the curvature perturbation $\mathcal{R}_k$ evaluated, in general, at the end of inflation.

3. Evolution of the curvature perturbations at super-Hubble scales

The equation (21) that describes the evolution of the curvature perturbations is completely equivalent to the equation of motion of an oscillator with the time-dependent damping term (z'/z). It is evident from this correspondence that the curvature perturbations can be expected to grow at super-Hubble scales (i.e. as $k \to 0$) if there exists a period during which the damping term proves to be negative [3, 4]. Actually, as we shall see, if (z'/z) turns out to be negative for some amount of time, then, for a certain range of modes, the amplitude of the curvature perturbations is enhanced at super-Hubble scales, while the amplitude of another range of modes is suppressed, when compared to their values at Hubble exit. We shall now outline as to how the quantity (z'/z) turns out to be negative for the tachyonic case during a period of fast roll inflation or when there is a break in inflation.

The slow roll approximation is an expansion in terms of small parameters that are defined as derivatives either of the potential $V(T)$ or the Hubble parameter H [15]. For our discussion, we shall make use of the horizon flow parameters which are defined as the derivatives of the Hubble parameter H with respect to the number of e-foldings N as follows [16]:

$$\epsilon_0 \equiv \left(\frac{H_*}{H}\right) \quad \text{and} \quad \epsilon_{i+1} \equiv \left(\frac{d\ln|\epsilon_i|}{dN}\right) = \left(\frac{\dot{\epsilon}_i}{H\,\epsilon_i}\right) \quad \text{for}\ \ i \geq 0, \tag{24}$$

where H_* is the Hubble parameter evaluated at some given time, and inflation occurs when $\epsilon_1 < 1$. It should be pointed out here that these functions form exactly the same hierarchy of inflationary flow equations as the Hubble slow roll parameters [15, 16].

For the case of the DBI scalar field we are considering here, the first two horizon flow functions are given by [14]

$$\epsilon_1 = \left(\frac{3\,\dot{T}^2}{2}\right) \quad \text{and} \quad \epsilon_2 = \left(\frac{2\,\ddot{T}}{H\,\dot{T}}\right). \tag{25}$$

We find that the quantity (z'/z) can be expressed in terms of these two horizon flow functions as follows:

$$\left(\frac{z'}{z}\right) = (a\,H)\,\left(1 + \left(\frac{\epsilon_2}{2}\right)\,\left[\frac{1}{1-(2\,\epsilon_1/3)}\right]\right). \tag{26}$$

It is apparent from this expression that, in the slow roll limit, i.e. when $(\epsilon_1, \epsilon_2) \ll 1$, $(z'/z) \simeq (a\,H) = \dot{a}$ which, in an expanding universe, is a positive definite quantity. Clearly, (z'/z) cannot be negative in the slow roll regime. However, note that (z'/z) can become negative if the following condition is satisfied:

$$\epsilon_2 < -2\left[1 - \left(\frac{2\,\epsilon_1}{3}\right)\right]. \tag{27}$$

Such a situation can occur either when there is a break in inflation, say, when $\epsilon_1 = 1$ and $\epsilon_2 < -(2/3)$ or during a period of fast roll inflation, i.e. when $\epsilon_1 \ll 1$ and $\epsilon_2 < -2$. In the following subsection, we shall discuss a specific example of the second scenario.

3.1. A specific example

To explicitly illustrate the phenomenon of the enhancement or the suppression of the amplitude of the curvature perturbations at super-Hubble scales, we shall work with the potential

$$V(T) = V_0\,\left(1 + V_1\,T^4\right), \tag{28}$$

where V_0 and V_1 are positive constants. For this potential, we find that, in the T-$\dot{T}$ plane, there exists only one finite critical point at $(T = 0,\, \dot{T} = 0)$ for the equation of motion (4). A linear stability analysis about this point immediately suggests that the critical point is a stable fixed point. This implies that, regardless of the initial conditions that the tachyon starts rolling from, it will always approach the critical point asymptotically. Also, we find that, all the trajectories in the phase space rapidly approach an attractor trajectory which has the following three regimes for the field evolution: $\dot{T} \ll 1$, $\dot{T} \lesssim 1$, and $\dot{T} \ll 1$ again. It is then clear from the expressions (25) for ϵ_1 and ϵ_2 that, as the field starts rolling down the potential from a large value, ϵ_1 can grow from a small value to some maximum value and then decrease to a small value again. Also, this behavior will allow ϵ_2 to become negative during the period when the field is decelerating—a feature that is necessary to achieve the condition (27). However, the minimum value attained by ϵ_2 and for how long it can remain negative depends on the values of the parameters V_0 and V_1 that describe the potential.

We now need to choose the values of the parameters V_0 and V_1 of the potential so that the condition (27) is satisfied. A general analysis in terms of the horizon flow functions is not possible without explicitly solving the equation of motion for T. Hence, instead of the horizon flow functions, we shall now make use of the potential slow roll parameters to estimate these values [17]. For the DBI scalar field we are considering here, the first two potential slow roll parameters are defined as [8]

$$\varepsilon_{\rm V} = \left(\frac{M_{\rm P}^2}{2}\right)\left(\frac{V_T^2}{V^3}\right) \quad \text{and} \quad \delta_{\rm V} = M_{\rm P}^2\left[3\left(\frac{V_T^2}{V^3}\right) - 2\left(\frac{V_{TT}}{V^2}\right)\right], \qquad (29)$$

where $V_{TT} \equiv (d^2V/dT^2)$. For $M_{\rm P}$ set to unity, we find that $\delta_{\rm V} < -2$ provided $V_1 > 0.036$‖.

We have solved the background equations and the equation describing the curvature perturbation numerically. The results that we present here are for the following values of the potential parameters: $V_0 = 0.5$ and $V_1 = 0.18$. We have chosen the standard initial conditions at sub-Hubble scales corresponding to the Bunch-Davies vacuum for the curvature perturbations. The initial conditions we have imposed are easily expressed in terms of the Mukhanov-Sasaki variable v_k that is related to the curvature perturbation through the relation: $v_k = (\mathcal{R}_k\, z)$. The initial conditions we have imposed are as follows (see, for instance, the second textbook in Ref. [1]):

$$v_k = \left(\frac{1}{2\,\omega_k}\right)^{1/2} \qquad \text{and} \qquad v_k' = -i\left(\frac{\omega_k}{2}\right)^{1/2}, \qquad (30)$$

where

$$\omega_k^2 = \left[(k\, c_{\rm S})^2 - (z''/z)\right], \qquad (31)$$

and we have imposed these conditions at a given time when all the modes of interest are well inside the Hubble radius.

In Figure 1, we have plotted the quantity (z'/z) as a function of the number of e-foldings N. It is clear from the figure that (z'/z) is negative during $58 < N < 61$. In Figure 2, we have plotted the amplitude of the curvature perturbation $\mathcal{R}_k$ as a function of N for two modes which are at super-Hubble scales when the slow roll to fast roll transition takes place. It is evident from the figure that, while the amplitude of $\mathcal{R}_k$ corresponding to the mode with wave number $k = 0.1$ is enhanced at super-Hubble scales, the amplitude of the mode with wave number $k = 0.03$ is suppressed at late times, when compared to their values at Hubble exit¶. We should mention that, to highlight these behaviors, we have chosen modes that exhibit sufficient amplification or

‖ Actually, the potential slow roll parameters and the horizon flow functions are of the same order only in the slow roll limit. Their equivalence will necessarily break down in the fast roll regime we are interested in. However, we find that the value for V_1 we shall work with (which is greater than 0.036) indeed leads to the required behavior.

¶ In Refs. [3, 4], the authors emphasize the point that, a period of deviation from slow-roll inflation can enhance the amplitude of the curvature perturbations at super-Hubble scales, but seem to overlook the fact that it can also lead to their suppression. Actually, they also encounter the suppression of the amplitude in the examples they consider. In Figures 1 and 2 of Ref. [4], they plot the power spectrum evaluated at the end of inflation as well as at a time soon after the modes leave the Hubble radius. It is

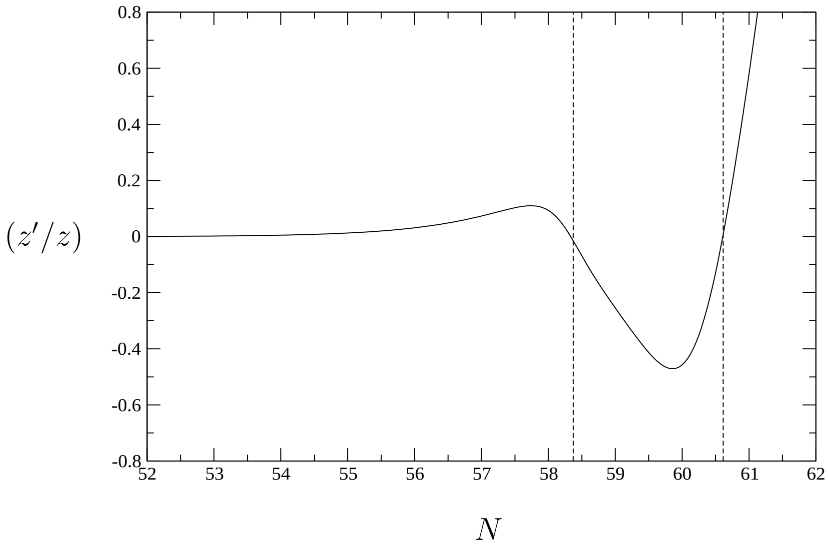

Figure 1. The evolution of the quantity (z'/z) has been plotted as a function of the number of e-folds N. The vertical lines indicate the regime where (z'/z) is negative. Note that it remains negative for a little less than three e-folds between N of 58 and 61.

suppression for the specific model and parameters we are considering here. Finally, we should also stress the point that, had there been no transition to the fast roll regime, the amplitude of the curvature perturbations would have frozen at their value at Hubble exit.

3.2. Entropy perturbations as the source of evolution at super-Hubble scales

In this subsection, we shall outline as to how the entropy perturbation $\mathcal{S}$ grows during the fast roll regime, and how such a growth in turn acts as the source for the change in the amplitude of the curvature perturbation at super-Hubble scales.

On using the expression (19) for the entropy perturbation $\mathcal{S}$, we find that the differential equations (14) and (21) describing the evolution of $\mathcal{R}$ can be written in Fourier space as the following two first order equations [3]:

$$\left(\frac{\mathcal{R}_k'}{aH}\right) = \mathcal{A}\,\mathcal{S}_k, \tag{32}$$

$$\left(\frac{\mathcal{S}_k'}{aH}\right) = \mathcal{B}\,\mathcal{S}_k - \mathcal{C}\,\left(\frac{k^2}{a^2H^2}\right)\,\mathcal{R}_k. \tag{33}$$

The quantities $\mathcal{A}$, $\mathcal{B}$ and $\mathcal{C}$ appearing in the above two equations can be expressed in terms of the first three horizon flow parameters as

$$\mathcal{A} = (3 - 2\,\epsilon_1)\,\left(\frac{3 - 6\,\epsilon_1 + \epsilon_2}{6 - 12\,\epsilon_1 + \epsilon_2}\right), \tag{34}$$

clear from these two figures that, while a certain range of modes are amplified at super-Hubble scales, another range of modes are suppressed.

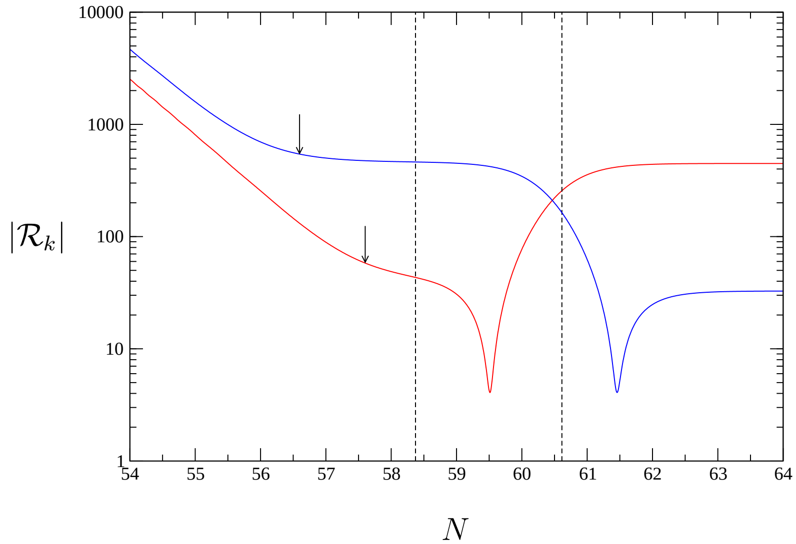

Figure 2. The evolution of the amplitude of the curvature perturbation $\mathcal{R}_k$ is plotted as a function of the number of e-folds N for the modes with wave numbers $k = 0.03$ (in blue) and $k = 0.1$ (in red). As in the previous figure, the vertical lines delineate the regime where (z'/z) is negative. The arrows indicate the time at which the modes leave the Hubble radius, i.e. when $(k\, c_{\rm S}) = (a\, H)$. Note that the amplitude of the curvature perturbation for the $k = 0.1$ mode is enhanced at super-Hubble scales (by a factor of about 10), while the amplitude of the $k = 0.03$ mode is suppressed (by a factor of about 20), when compared to their values at Hubble exit. We should mention that these two particular modes have been chosen for the reason that, in the specific example that we are considering, they exhibit sufficient extent of amplification or suppression at super-Hubble scales.

$$\begin{aligned}
\mathcal{B} = & \left(\frac{1}{(3-2\epsilon_1)\,(6-12\,\epsilon_1+\epsilon_2)\,(3-6\,\epsilon_1+\epsilon_2)}\right)\\
& \times\biggl[\left(2\,\epsilon_1\epsilon_2\,\left[3-72\,\epsilon_1^2+\epsilon_2\,(12+\epsilon_2)-6\,\epsilon_1\,(12+2\,\epsilon_2+\epsilon_3)\right]-9\,\epsilon_2\epsilon_3\right)\\
& \qquad -(6-12\,\epsilon_1+\epsilon_2)\,(3-6\,\epsilon_1+\epsilon_2)\,\left(9-9\,\epsilon_1+3\,\epsilon_2+2\,\epsilon_1^2\right)\biggr],
\end{aligned} \tag{35}$$

$$\mathcal{C} = \left(\frac{1}{3}\right)\,\left(\frac{6-12\,\epsilon_1+\epsilon_2}{3-6\,\epsilon_1+\epsilon_2}\right), \tag{36}$$

with the third parameter ϵ_3 given by

$$\epsilon_3 = \left(\frac{1}{H}\right)\,\left[\left(\frac{\dddot{T}}{\ddot{T}}\right)-\left(\frac{\ddot{T}}{\dot{T}}\right)-\left(\frac{\dot{H}}{H}\right)\right]. \tag{37}$$

We shall now make use of the coupled first order differential equations (32) and (33) to understand the evolution of the entropy perturbations at super-Hubble scales and its effect on the curvature perturbations during the slow roll and the fast roll regimes.

Let us first discuss the behavior in the slow roll regime. During slow roll, we can ignore the horizon flow parameters when compared to the numerical constants in the above expressions for $\mathcal{A}$, $\mathcal{B}$ and $\mathcal{C}$. Since we are interested in the evolution at super-Hubble scales, one would be tempted to ignore the term involving $\mathcal{R}_k$ in Eq. (33). If we can indeed do so, we can immediately conclude that $\mathcal{S}_k \propto e^{-3N}$ during an epoch of slow roll inflation. However, the self-consistent numerical solutions we have obtained to equations (32) and (33) indicate otherwise. In Figure 3, using the numerical solutions to the curvature perturbations $\mathcal{R}_k$ we had discussed in the last section and the relation (32), we have plotted the evolution of the entropy perturbation $\mathcal{S}_k$ for the two modes $k = 0.03$ and $k = 0.1$ as a function of the number of e-folds. It is clear from the figure that while there is indeed an intermediate period in the slow roll phase when $\mathcal{S}_k \propto e^{-3N}$, the late time behavior actually has the form $\mathcal{S}_k \propto e^{-2N}$. In fact, we find that all the modes that leave the Hubble radius before the transition to fast roll exhibit such a behavior. We should point out here that similar conclusions have been arrived at earlier for the case of perturbations induced by the canonical scalar field [3].

During a period of fast roll inflation, in contrast to the slow roll case, we cannot ignore the horizon flow parameters in the quantities $\mathcal{A}$, $\mathcal{B}$ and $\mathcal{C}$. If we now choose to neglect the term involving $\mathcal{R}_k$ in Eq. (33), we find that the equation reduces to

$$\left(\frac{\mathcal{S}_k'}{aH}\right) \simeq (\mathcal{B}\,\mathcal{S}_k)\,. \tag{38}$$

Moreover, we find that, on using the background equations, we can rewrite the expression (37) for ϵ_3 as follows:

$$\epsilon_3 = -\left(\frac{3}{2}\right) + \left(\frac{7\,\epsilon_1}{2}\right) - \left(\frac{\epsilon_2}{4}\right) - \left(\frac{\epsilon_1\,\epsilon_2}{2(3-2\epsilon_1)}\right) + \left(\frac{3\,\epsilon_1}{\epsilon_2}\right) - \left(\frac{V_{TT}}{V\,H^2}\right)\left(\frac{1}{\epsilon_2}\right)\left[1 - \left(\frac{2\,\epsilon_1}{3}\right)\right]. \tag{39}$$

If we now assume that $\epsilon_1 \ll 1$ and make the additional assumption that $(V_{TT}/V\,H^2) \ll 1$[+], we find that ϵ_3 simplifies to [3]

$$\epsilon_3 \simeq -\left(\frac{3}{2}\right) - \left(\frac{\epsilon_2}{4}\right). \tag{40}$$

On substituting this value in the expression (35) for $\mathcal{B}$ and assuming that $\epsilon_2 \simeq -5$ (which is roughly the largest value of ϵ_2 in the fast roll regime for our choice of parameters), we obtain that

$$\mathcal{S}_k \propto e^{4N}. \tag{41}$$

As we have illustrated in Figure 3, this rough estimate is corroborated by the numerical result we obtain. It is then evident from equation (32) that it is such a rapid growth of the entropy perturbation during the fast roll regime (instead of a slow roll decay) that is responsible for the change in the amplitude of the curvature perturbation at super-Hubble scales. However, we should add that a rapid growth of entropy perturbations

[+] We should point out here that, for the case of the standard scalar field, the quantity (V_{TT}/H^2) is actually the second potential slow roll parameter. However, for the DBI field, the equivalent quantity turns out to be $(V_{TT}/V\,H^2)$, and the extra factor of V in the denominator is due to the form of the DBI action.

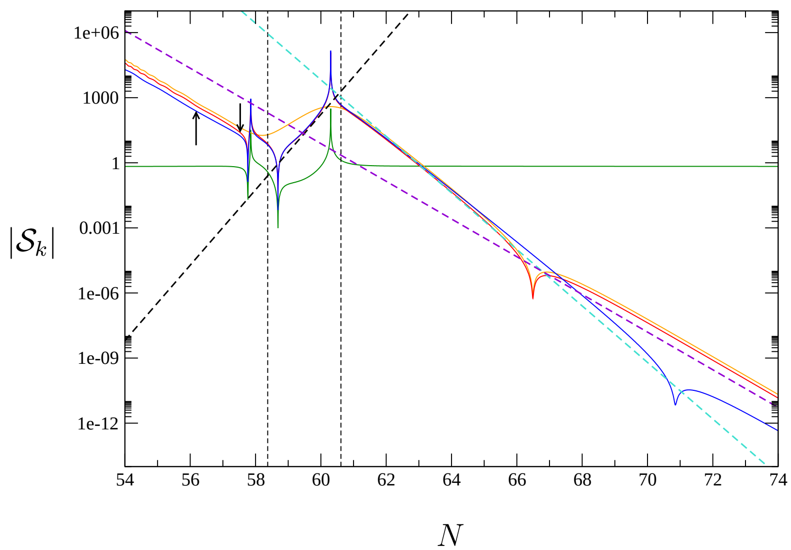

Figure 3. The evolution of the amplitude of the entropy perturbation $\mathcal{S}_k$ is plotted as a function of the number of e-folds N for the two modes $k = 0.03$ (in blue) and $k = 0.1$ (in red) we had considered in the previous figure. The dashed lines in black, turquoise and violet indicate the $e^{(4N)}$, $e^{-(3N)}$ and $e^{-(2N)}$ behavior, respectively. The vertical lines again delineate the fast roll regime and, as before, the arrows indicate the time at which the modes leave the Hubble radius. We have also plotted the quantities $(1/\mathcal{A})$ (in green) and $(|\mathcal{R}_k'|/a\,H)$ (in orange) for the mode $k = 0.1$. The former is discontinuous while the latter is continuous, and it is the former quantity that leads to the discontinuities in the evolution of $\mathcal{S}_k$. The conclusions we have discussed in the text—the $e^{(4N)}$ growth of the entropy perturbation during fast roll, the intermediate $e^{-(3N)}$ slow roll behavior and the late time $e^{-(2N)}$ slow roll decay—are evident from the figure. It is also important to note that the entropy perturbations associated with both the modes evolve in a similar fashion during the fast roll phase.

is exhibited only by modes that leave the Hubble radius just before the transition to the fast roll phase. We find that the earlier the modes leave the Hubble radius, less rapidly do their entropy perturbations grow during the fast roll phase. Evidently, the longer a mode has been outside the Hubble radius before the fast roll transition, the more suppressed the entropy perturbation is, and lesser is its growth during the fast roll phase. Therefore, its ability to affect the curvature perturbation gets suppressed correspondingly.

The following clarifying remarks are in order at this stage of our discussion. To begin with, we should reiterate the point we had made earlier, viz. that, in the absence of a transition to the fast roll regime, the amplitude of the curvature perturbations would have frozen at their value at Hubble exit. Also, since, at sub-Hubble scales, the modes do not feel the effect of the background quantities, the transition has virtually no effect on those modes that are well within the Hubble radius during the period of fast roll inflation. In fact, the fast roll regime has the maximum effect on the modes that leave the Hubble radius just before the transition. (As we mentioned, it is for this reason that, in Figures 2 and 3, we have chosen modes that leave the Hubble scale just before the transition to the fast roll regime takes place and which exhibit sufficient extent of amplification or suppression.) While the amplitude of a certain range of modes is indeed enhanced at super-Hubble scales as has been noticed earlier in the case of the canonical scalar field [3], we find that, actually, there also exists a range of modes whose amplitude is *suppressed* at super-Hubble scales, when compared to their value at Hubble exit. This is evident from Figure 5 wherein we have plotted the power spectrum evaluated soon after Hubble exit as well as the spectrum computed at the end of inflation. Moreover, the extent of the change in the amplitude of the curvature perturbations proves to be smaller and smaller for modes that leave the Hubble radius earlier and earlier before the transition. Clearly, this is due to the combined effect of the slower growth during the fast roll phase and the exponential suppression of the entropy perturbations far outside the Hubble radius.

4. The long wavelength approximation

In the previous section, working in the fluid picture, we had discussed as to how the growth of entropy perturbations acts as the source for the evolution of the curvature perturbations at super-Hubble scales during a period of fast roll inflation. In this section, extending the earlier result for the canonical scalar field [4], we evaluate the power spectrum in the long wavelength approximation and show that it matches the exact spectrum obtained numerically, quite well. Since the analysis for the DBI field is essentially similar to that of the canonical scalar field, rather than repeat the discussion, we shall simply point out the difference between the two cases and present the final results.

As far as the evolution of the curvature perturbation goes, the only difference between the canonical and the DBI scalar fields is the factor of $c_{\rm s}^2$ that appears as the coefficient of k^2 in Eq. (21). The effective speed of sound $c_{\rm s}$ turns out to be unity for the standard scalar field. In the earlier analysis for the canonical scalar field [4], the amplitude of curvature perturbation at the end of inflation was related to its value soon after Hubble exit in terms of quantities involving the function z at the $\mathcal{O}(k^2)$ in the long wavelength approximation. Therefore, the corresponding result for the DBI scalar field essentially involves suitably replacing the quantity k^2 with $(k^2\, c_{\rm s}^2)$. We find that, at the $\mathcal{O}(k^2)$, the amplitude of the curvature perturbation at the end of inflation, say, at η_*, can be related to its amplitude soon after Hubble exit, say, at η_k, by the following relation:

$$\mathcal{R}_k(\eta_*) = \left[\alpha_k\, \mathcal{R}_k(\eta_k)\right], \tag{42}$$

where α_k is given by

$$\alpha_k = \left[1 + D_k(\eta_k) - F_k(\eta_k)\right]. \tag{43}$$

The quantities D_k and F_k in the above expression for α_k are described by the following integrals involving the functions $z(\eta)$ and $c_{\rm S}(\eta)$:

$$D_k(\eta) \simeq \mathcal{H}_k \int\limits_{\eta}^{\eta_*} d\eta_1 \, \left(\frac{z^2(\eta_k)}{z^2(\eta_1)}\right) \tag{44}$$

and

$$F_k(\eta) \simeq k^2 \int\limits_{\eta}^{\eta_*} \frac{d\eta_1}{z^2(\eta_1)} \int\limits_{\eta_k}^{\eta_1} d\eta_2 \, \left[c_{\rm S}^2(\eta_2)\, z^2(\eta_2)\right] \tag{45}$$

with $\mathcal{H}_k$ denoting the conformal Hubble parameter evaluated at η_k.

As we had pointed out before, during slow roll inflation, $(z'/z) \simeq (a\,H) = \dot{a}$. In other words, in the slow roll regime, z is a monotonically increasing quantity. Therefore, in such a regime, the quantity D_k remains small and the contribution due to F_k—since it is proportional to k^2—can be ignored at extreme super-Hubble scales. However, the contributions due to these two terms cannot be neglected if these quantities turn out to be larger than unity. Recall that $c_{\rm S}^2 = (1 - \dot{T}^2)$ and, hence, $0 \leq c_{\rm S}^2 \leq 1$. It is then clear from the above integrals for D_k and F_k that they can be large if, for a given mode, there exists an epoch during which $z(\eta)$ at super-Hubble scales is much smaller than the corresponding value when the mode left the Hubble radius. We find that indeed such a situation arises during the fast roll regime in the specific example we had discussed in the last section. For the potential and the parameters we were working with, we find that $0.65 < c_{\rm S}^2 < 1$. And, in Figure 4, we have plotted the quantity z^2 as a function of the number of e-foldings. It is the dip in the quantity z^2 during the fast roll regime that turns out to be responsible for the change in the amplitude of the curvature perturbation at super-Hubble scales.

In Figure 5, using the numerical integration of the modes we had discussed in the last section, we have plotted the power spectrum evaluated at the end of inflation as well as the spectrum that has been obtained in the long wavelength approximation using the relation (42). We have also plotted the power spectrum evaluated soon after the modes leave the Hubble radius. The figure clearly illustrates the following three points. Firstly, the spectrum evaluated at the $\mathcal{O}(k^2)$ in the long wavelength limit proves to be quite a good fit of the actual spectrum. Secondly, there is a considerable difference between the power spectrum that has been evaluated at the end of inflation and the spectrum that has been evaluated soon after Hubble exit. The difference is, in particular, large for the modes that leave the Hubble radius just before the fast roll regime. Thirdly, while the amplitude of the modes at super-Hubble scales in the wave number range $0.01 \lesssim k \lesssim 0.04$ is suppressed when compared to its value soon after Hubble exit, the amplitude of the modes in the range $0.04 \lesssim k \lesssim 0.1$ is enhanced.

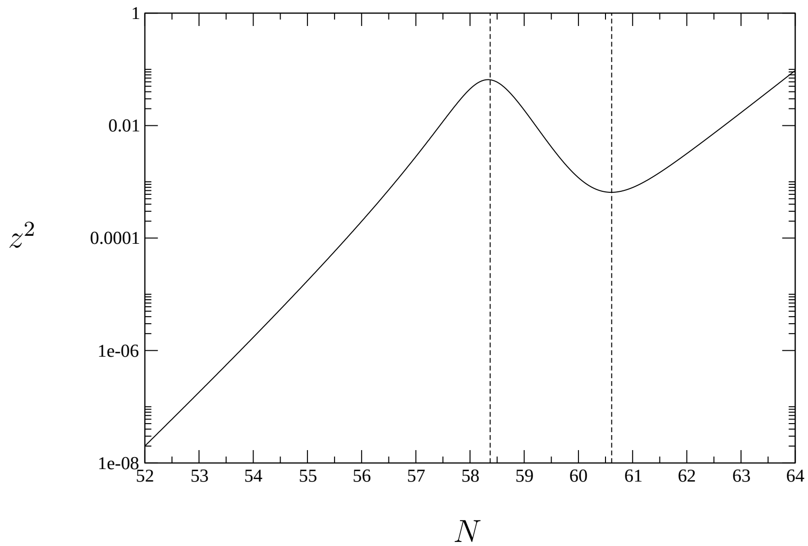

Figure 4. The evolution of the quantity z^2 is plotted as a function of the number of e-folds N. Note the dip during the fast roll regime that is outlined by the vertical lines. It is this dip that is responsible for (z'/z) being negative, which in turn leads to the change in the amplitude of the curvature perturbations at super-Hubble scales.

5. Summary

In this work, with the help of a specific example, we have shown that the amplitude of the curvature perturbations induced by a DBI scalar field can be *enhanced or suppressed* at super-Hubble scales if there exists a period of deviation from slow roll inflation. Working in the fluid picture, we have illustrated that, as in the case of the canonical scalar field, the change in the amplitude of the curvature perturbations arises due to the growth of the entropy perturbations in the fast roll regime. Moreover, following the results obtained earlier for the standard scalar field, we have shown that the power spectrum evaluated in the long wavelength approximation matches the exact spectrum obtained numerically very well.

Transitions from slow roll to fast roll inflation lead to deviations from a nearly scale-invariant power spectrum. The possibility that specific deviations from the standard scale independent power spectrum may fit the cosmic microwave background observations better have been explored recently in the literature [18, 19]. If we can systematically understand the effects of the quantity z on the curvature perturbation $\mathcal{R}_k$, we will be able to fine tune the transitions such as the ones we have discussed in this work to obtain the desired features in the power spectrum (in this context, see Ref. [19]). For instance, the sharp drop in the power spectrum in our model in the wavelength range $0.03 \lesssim k \lesssim 0.1$ may provide a better fit to the lower power observed in the quadrupole moment of the cosmic microwave background [20]. We are currently investigating these issues.

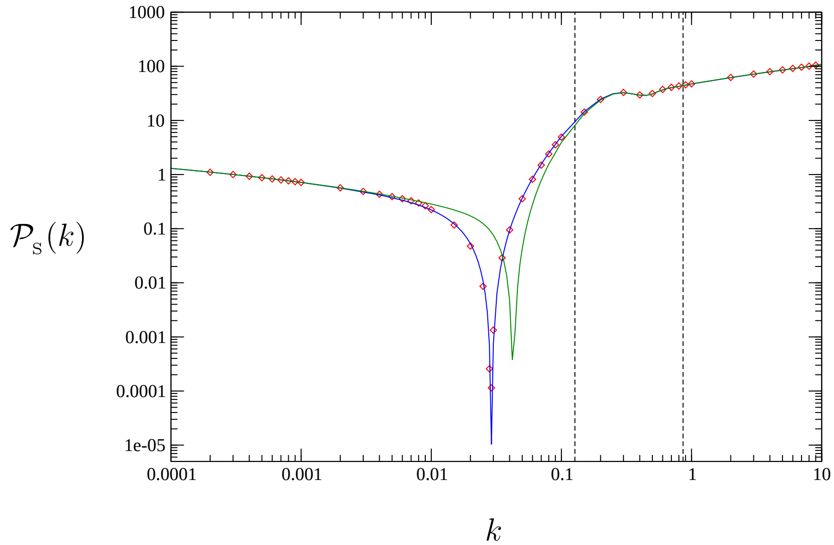

Figure 5. Plots of the scalar power spectrum that has been evaluated at the end of inflation through the numerical integration of the modes (in blue) as well as the spectrum that has been obtained using the long wavelength approximation (in red). The spectrum evaluated soon after the modes leave the Hubble radius (when $(k\, c_{\rm S}/a\, H) = 0.1$) has also been plotted (in green). The modes within the vertical lines leave the Hubble radius during the fast roll regime. It is clear from the figure that the power spectrum evaluated in the long wavelength approximation agrees quite well with the actual spectrum. However, there is a substantial difference between the power spectrum evaluated near Hubble exit and the spectrum evaluated at the end of inflation. The difference is, in particular, large for those modes whose Hubble exit occurs just before the period of fast roll inflation. Note that, while the amplitude of the modes at super-Hubble scales in the wave number range $0.01 \lesssim k \lesssim 0.04$ is suppressed when compared to its value near Hubble exit, the amplitude of the modes in the range $0.04 \lesssim k \lesssim 0.1$ is enhanced. Essentially, the valley in the power spectrum computed near Hubble exit has shifted towards smaller k when the spectrum is evaluated in the super-Hubble limit.

Acknowledgments

The authors would wish to thank Kim Juhan, T. Padmanabhan, S. Shankaranarayanan and K. P. Yogendran for discussions. We would also like to acknowledge the use of the cluster computing facility at the Harish-Chandra Research Institute (HRI), Allahabad, India. PC would also like to thank HRI for hospitality where part of this work was carried out.

References

[1] A. R. Liddle and D. H. Lyth, *Cosmological Inflation and Large-Scale Structure* (Cambridge University Press, Cambridge, England, 1999); V. F. Mukhanov, *Physical Foundations of Cosmology* (Cambridge University Press, Cambridge, England, 2005).

[2] H. Kodama and M. Sasaki, Prog. Theor. Phys. Suppl. **78**, 1 (1984); V. F. Mukhanov, H. A. Feldman and R. H. Brandenberger, Phys. Rep. **215**, 203 (1992); J. E. Lidsey, A. Liddle, E. W. Kolb, E. J. Copeland, T. Barreiro and M. Abney, Rev. Mod. Phys. **69**, 373 (1997); B. Bassett, S. Tsujikawa and D. Wands, Rev. Mod. Phys. **78**, 537 (2006).

[3] S. M. Leach and A. R. Liddle, Phys. Rev. D **63**, 043508 (2001).

[4] S. M. Leach, M. Sasaki, D. Wands and A. R. Liddle, Phys. Rev. D **64**, 023512 (2001).

[5] A. Sen, JHEP **9910**, 008 (1999); M. Garousi, Nucl. Phys. B **584** 284, (2000); E. Bergshoeff, M. de Roo, T. de Wit, E. Eyras and S. Panda, JHEP **0005**, 009 (2000); J. Kluson, Phys. Rev. D **62**, 126003 (2000).

[6] A. Sen, JHEP **04**, 048 (2002); *ibid.* **07**, 065 (2002).

[7] F. Quevedo, Class. Quant. Grav. **19**, 5721 (2002); K. Enqvist, A. Jokinen, A. Mazumdar, T. Multamaki and A. Vaihkonen, JCAP 0503, 010 (2005); K. Enqvist, A. Jokinen, A. Mazumdar, T. Multamaki and A. Vaihkonen, JHEP 08, 084 (2005).

[8] P. Chingangbam, S. Panda and A. Deshamukhya, JHEP **0502**, 052 (2005).

[9] M. R. Garousi, JHEP **12**, 036 (2003).

[10] M. R. Garousi, M. Sami and S. Tsujikawa, Phys. Rev. D **70**, 043536 (2004); M. R. Garousi, M. Sami and S. Tsujikawa, Phys. Lett. B **606**, 1 (2005); M. R. Garousi, M. Sami and S. Tsujikawa, Phys. Rev. D **71**, 083005 (2005); P. Chingangbam and T. Qureshi, Int. J. Mod. Phys. A **20**, 6083 (2005).

[11] C. Armendariz-Picon, T. Damour and V. F. Mukhanov, Phys. Lett. B **458**, 209 (1999); J. Garriga and V. F. Mukhanov, Phys. Lett. B **458**, 219 (1999).

[12] M. Sasaki, Prog. Theor. Phys. **70**, 394 (1983); *ibid.* **76**, 1036 (1986).

[13] C. Gordon, D. Wands, B. A. Bassett and R. Maartens, Phys. Rev. D **63**, 023506 (2001).

[14] D. A. Steer and F. Vernizzi, Phys. Rev. D **70**, 043527 (2004).

[15] A. R. Liddle, P. Parsons and J. D. Barrow, Phys. Rev. D **50**, 7222 (1994).

[16] D. J. Schwarz, C. A. Terrero-Escalante, A. A. Garcia, Phys. Lett. B **517**, 243 (2001).

[17] D. Roberts, A. R. Liddle, and D. H. Lyth, Phys. Rev. D **51**, 4122 (1995).

[18] C. R. Contaldi, M. Peloso, L. Kofman and A. Linde, JCAP **0307**, 002 (2003); G. Nicholson, C. R. Contaldi, astro-ph/0701783.

[19] L. Covi, J. Hamann, A. Melchiorri, A. Slosar and I. Sorbera, Phys. Rev. D **74**, 083509 (2006); J. Hamann, L. Covi, A. Melchiorri and A. Slosar, Phys. Rev. D **76**, 023503 (2007).

[20] A. Shafieloo and T. Souradeep, Phys. Rev. D **70**, 043523 (2004); A. Shafieloo, T. Souradeep, P. Manimaran, P. K. Panigrahi and R. Rangarajan, Phys. Rev. D **75**, 123502 (2007).